Direct femtosecond laser nanopatterning of glass substrate by particle-assisted near-field enhancement

Y. Zhou, M. H. Hong, JYH Fuh, L. Lu, B. S. Luk'yanchuk, Z. B. Wang, L. P. Shi, and T. C. Chong

Citation: Applied Physics Letters **88**, 023110 (2006); doi: 10.1063/1.2163988
View online: http://dx.doi.org/10.1063/1.2163988
View Table of Contents: http://scitation.aip.org/content/aip/journal/apl/88/2?ver=pdfcov
Published by the AIP Publishing

Direct femtosecond laser nanopatterning of glass substrate by particle-assisted near-field enhancement

Y. Zhou
Department of Mechanical Engineering, National University of Singapore, 2 Engineering Drive 3, Singapore 117576 and Data Storage Institute, 5 Engineering Drive 1, Singapore 117608

M. H. Hong[a)]
Data Storage Institute, 5 Engineering Drive 1, Singapore 117608 and Department of Electrical and Computer Engineering, National University of Singapore, 4 Engineering Drive 3, Singapore 117576

JYH Fuh and L. Lu
Department of Mechanical Engineering, National University of Singapore, 2 Engineering Drive 3, Singapore 117576

B. S. Luk'yanchuk, Z. B. Wang, L. P. Shi, and T. C. Chong
Data Storage Institute, 5 Engineering Drive 1, Singapore 117608

(Received 30 August 2005; accepted 1 December 2005; published online 11 January 2006)

Direct femtosecond laser nanopatterning of glass substrate by particle-assisted near-field enhancement was demonstrated in this letter. The nanostructure was characterized by field-emission scanning electron microscopy and atomic force microscopy. No cracks were found on the glass surface. The hole size were measured from 200 ~ 300 nm. When laser fluence is close to the damage threshold, a trihole structure was observed. Nonlinear multiphoton absorption and near-field enhancement were the mechanisms of the nanofeature formation. Calculations based on particle-on-surface theory were carried out. The suggested method has potential applications in the nanolithography of a transparent glass substrate for nanostructure device fabrication. © *2006 American Institute of Physics*. [DOI: 10.1063/1.2163988]

Glass is widely used in novel device packaging, microoptics, and biomedical devices due to its outstanding chemical and optical properties.[1] However a high structure resolution is required in the applications of the nanoengineering and information industries. It leads to many investigations on the sophisticated fabrication methods of glass nanostructure devices, such as nanoimprinting,[2] electron beam lithography,[3] and chemical etching. In general, glass is hard, brittle, and nonconductive. Therefore, it is a high challenge to process glass by conventional methods. Laser microprocessing is an attractive approach in glass engineering. However, the minimum feature size is determined by the diffraction limit of light. Recently, optical near-field lithography has been developed as a new technology to overcome the diffraction limit by a particle mask.[4]

Another possible method to overcome the limitation is by femtosecond laser irradiation. This laser can provide extremely high peak power intensity for nonlinear and multiphoton absorption by the substrate materials. Furthermore, nonlinear absorption of femtosecond laser irradiation can result in an increase in the refractive index at the focal point inside the glass, which is potentially effective to produce nanofeatures.[5] In this letter, nanocrater formation was studied by combining a particle mask and femtosecond laser irradiation. By depositing a monolayer of microspheres on the substrate surface as a particle mask and utilizing a femtosecond laser as a light source, nanoscale holes can be created.[6] It is proposed that nonlinear absorption and optical near-field enhancement play important roles in nanocrater formation on glass substrate.

Glass substrate was cleaned with acetone in an ultrasonic bath for 5 min followed by rinsing in deionized (DI) water and then dried by N_2 gas (purity 99.999%). The spherical silica particles (Duke, $n=1.6$, 10% size deviation) with the diameter of 1 μm were applied on the glass substrate after the suspension had been diluted with DI water. The substrate was kept still until all the water had been evaporated. As a result, a silica monolayer array was formed on the substrate surface.

A Ti:sapphire (Spectra Physics Tsunami, Mode 3960) and a regenerative amplifier (Spectra Physics Spitfire, Mode 9769A) were used as the light source (wavelength $\lambda=800$ nm, pulse duration $\tau=100$ fs and repetition rate from 1 to 1000 Hz). The laser was focused by a 20× microscope objective lens mounted on a Z stage. The laser spot size is about 5.4 μm. The laser was incident normally on the substrate surface. After the exposure the sample was characterized by atomic force microscopy (AFM; Digital Instruments D3000) and field-emission scanning electron microscopy (SEM; Hitachi S-4100).

Figure 1(a) shows a typical nanohole array created on the glass substrate after femtosecond laser shot at a laser fluence of 35 J/cm^2. As can be seen, the silica particles on the glass surface were removed after the laser irradiation, and nanostructures were formed at the place where the particles were originally located. Meanwhile, debris was observed around the nanocrater. They are hard to remove by the conventional ultrasonic cleaning method due to strong adhesion. The cross section of craters is shown in Fig. 1(b). The full width at half-maximum is about 250 nm and average depth of nanofeatures is around 150 nm. The size of melting zone

[a)]Author to whom correspondence should be addressed; electronic mail: Hong_Minghui@dsi.a-star.edu.sg

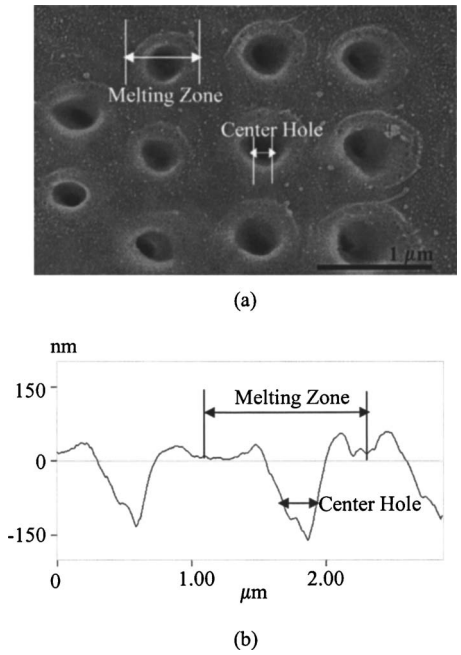

FIG. 1. (a) SEM image of nanocraters formed under 1.0 μm silica particles on glass surface by 800 nm, 100 fs laser pulse irradiation at a laser fluence of 35 J/cm^2. (b) AFM image of cross-sectional view of craters.

ranges from 380 to 650 nm. It is observed that the edges of these nanostructures are free of cracks. This can be contributed to the ultrashort laser pulse. For long-pulse-duration laser the formation of cracks was caused mainly by laser associated high temperatures and high pressure.[7] Processing with ultrashort laser pulses essentially eliminates the heat flow to the surrounding material. Therefore, thermally induced substrate cracking is prevented.

To further investigate the influence of laser fluence on the formation of the nanocrater, we repeated the experiments with different laser fluences. Figure 2 shows the SEM images of nanopatterns on a glass surface by laser irradiation on a particle mask with a fluence ranging from 17.5 to 61.3 J/cm^2. From Figs. 2(a) and 2(b) the nanopatterning shape does not change too much as the laser fluence increases from 17.5 to 26.3 J/cm^2. They are single-hole structures. In Fig. 1(a) the nanocrater formed at a laser fluence of 35 J/cm^2 has been shown. It was found that the center-hole size was enlarged. However, the melting zones of the patterns were kept the same size. A further increase of the laser fluence led to a very interesting phenomenon: at the laser fluence of 43.8 J/cm^2, there were three linked holes inside each nanocrater, as shown in Fig. 2(c). It was referred to as trihole crater. Compared to those structures at the lower laser fluence, the main difference is that there are two wing holes formed on both sides of the center hole. And the melting zone increases from 450 to 800 nm. The trihole nanocrater became prominent as laser fluence increased further to 52.5 J/cm^2 [as shown in Fig. 2(d)]. The two wing holes grew much bigger while the center hole changed from the original circular to elliptical shape. Meanwhile, the melting zone was also elliptical in shape. The orientation of the major axis of the nanocrater was perpendicular to the nanohole major axis. When the fluence increased further to 61.3 J/cm^2, the whole area was damaged, as shown in Fig. 2(e). In contrast, glass substrate without a particle mask was irradiated at the same laser fluence. No damage was observed. This shows

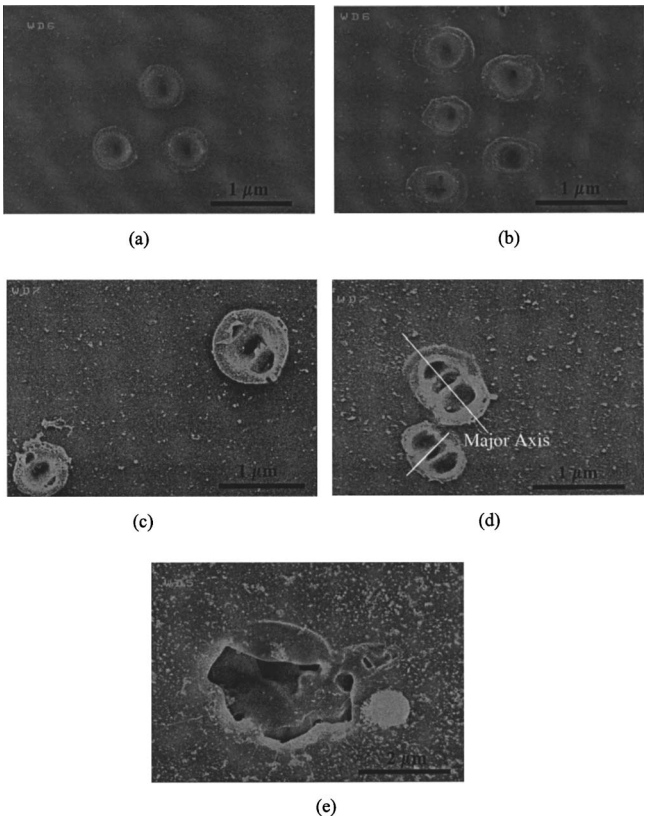

FIG. 2. SEM images of the patterns on the glass substrate after the laser irradiation at different laser fluences of (a) 17.5 J/cm^2, (b) 26.3 J/cm^2, (c) 43.8 J/cm^2, (d) 52.5 J/cm^2, and (e) 61.3 J/cm^2.

that particle-assisted near-field enhancement is the main mechanism for the formation of nanocrater.

Figure 3 is the relationship between the sizes of the center holes and the melting zone as functions of laser fluence. Both center holes and melting zone sizes increased with the laser fluence, but the melting zone increased faster than the center holes. At high laser fluence, the melting zone can be as large as the particle size of 1 μm, while the diameter of the center hole remains at about 300 nm.

In order to explain these results, the interaction between an ultrashort laser and transparent glass materials has to be analyzed. Electrons absorb photon energy and consequently

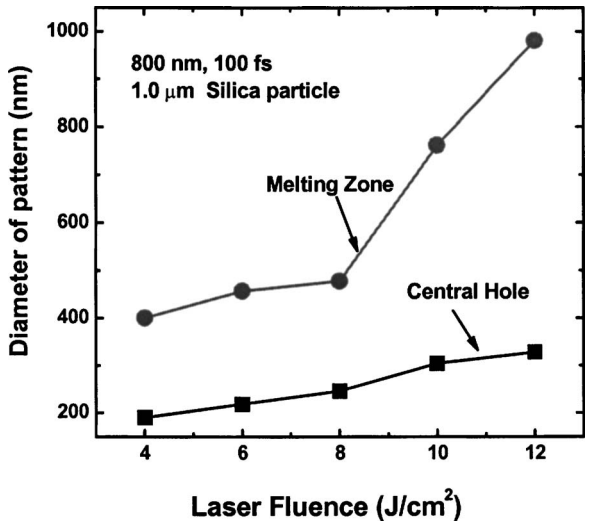

FIG. 3. Average size of nanocraters as a function of laser fluence.

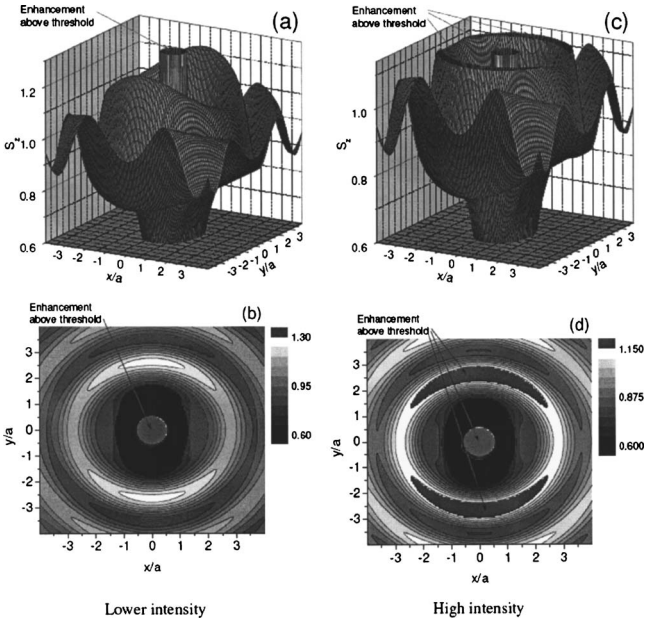

FIG. 4. Calculated enhancement in intensity distribution (z component of the Poynting vector), $S_z=I/I_0$, on the glass surface under a 1.0 μm silica particles ($n=1.5$ for $\lambda=800$ nm). Three-dimensional pictures (a) and (c) present intensity distributions, where the top of the pictures corresponds to certain threshold for slightly different input intensity I_0. The same distributions are also shown in contour plots (b) and (d). The right pictures corresponds to input intensity I_0, which is 13% higher than input intensity I_0 in the left pictures.

transfer the energy to lattices in a very short time that is generally in the time scale of several tens of picoseconds[8] in the condition of long pulse exposure. However, multiphoton absorption often takes place for the femtosecond laser pulse interaction with glass. The n-photon absorption is proportional to the nth power of the intensity.[9] This effect significantly narrows the processed area. As a result, with femtosecond lasers, the processing area should be confined in the central part of the optical axis[9] Furthermore, femtosecond laser-induced nonlinear effect gives rise to the change of glass optical properties affecting the propagation of incident light.[5,10] The laser beam was then self-focused in smaller area and extremely high laser fluence formed nanoscale feature size on glass.

Besides these effects, the near-field enhancement due to light scattering by the small spherical transparent particle plays an important role as well. The distribution of laser intensity can be found from the particle-on-surface theory.[11,12] We used a fast algorithm of reflected matrix calculation, suggested in Ref. 13. In Fig. 4 the normalized distribution of the z component of the Poynting vector (optical enhancement $S_z=I/I_0$) is shown. Here I_0 is the input laser intensity. Parameters that were used in calculations correspond to the experiment: particle diameter $2a=1$ μm, laser wavelength $\lambda=800$ nm, and refraction index for particle and glass $n=1.5$. One can see from Fig. 4 that maximal laser intensity is localized within a small region near the particle-substrate contacting point and the size of this central region of enhanced intensity is about 300 nm in good agreement with experimental measurements. Modification of the hole shape can be qualitatively understood considering some threshold intensity $I>I_{\mathrm{tr}}$ necessary to produce hole structure. With higher input intensity I_0 the modification of the holes structure appears at smaller $S_z=I_{\mathrm{tr}}/I_0$ value. One can see from Figs. 4(a) and 4(b) that a single crater is created at small intensity, while with higher intensity the trihole structure has to be created [see Figs. 4(c) and 4(d)]. In experiment we saw the whole region destroyed at high fluences [see Fig. 2(e)]. Pattern of the intensity distribution under the particle was discussed previously in Refs. 12–15. We should mention also that the maximal intensity is quite sensitive to the particle size; small variations in size parameter can lead to large variations in this intensity. It can be clearly seen in Fig. 1, where variation in the craters size was bigger 30% although variation of the particle size was smaller 10%.

In summary, nanocraters were created on a glass surface by 800 nm fs laser irradiation of self-assembled 1 μm silica particle mask. No cracks were found at edges of produced nanostructures on the glass surface. At low fluence the feature sizes were found from 200 to 300 nm with the average depth of 150 nm. At high fluence trihole structure was created when laser fluence was larger than 43.8 J/cm^2. Nanostructure formation can be attributed to two main reasons: (1) nonlinear effect arising from the interaction of femtosecond laser pulse with transparent glass substrate, and (2) optical near-field enhancement due to light scattering by the transparent silica particles. It provides a potential approach to achieve no crack nanofabrication of glass substrate.

The authors thank G. X. Chen and N. Doris for their invaluable advice.

[1] G. Geiger, Am. Ceram. Soc. Bull. **69**, 1131 (1990).
[2] S. Y. Chou, P. R. Krauss, and P. J. Renstrom, J. Vac. Sci. Technol. B **14**, 4129 (1996).
[3] J. R. Wendt, G. A. Vawter, R. E. Smith, and M. E. Warren, J. Vac. Sci. Technol. B **13**, 2705 (1995).
[4] H. Schmid, H. Biebuyck, and B. Michel, Appl. Phys. Lett. **72**, 2379 (1998).
[5] S. Theppakuttai and S. C. Chen, Appl. Phys. Lett. **83**, 758 (2003).
[6] S. M. Huang, M. H. Hong, B. S. Luk'yanchuk, Y. W. Zheng, W. D. Song, Y. F. Lu, and T. C. Chong, J. Appl. Phys. **92**, 2495 (2002).
[7] Y. Kanemitsu and Y. Tanaka, J. Appl. Phys. **62**, 1208 (1987).
[8] S. I. Anisimov and B. S. Luk'yanchuk, Phys. Usp. **45**, 293 (2002).
[9] K. Piglmayer, R. Denk, and D. Bäuerle, Appl. Phys. Lett. **80**, 4693 (2002).
[10] K. H. Davis, K. Miura, N. Sugimoto, and K. Hirao, Opt. Lett. **21**, 1729 (1996).
[11] P. A. Bobbert and J. Vlieger, Physica A **137**, 209 (1986).
[12] S. M. Huang, Z. Sun, B. S. Luk'yanchuk, M. H. Hong, and L. P. Shi, Appl. Phys. Lett. **86**, 161911 (2005).
[13] Z. B. Wang, M. H. Hong, B. S. Luk'yanchuk, Y. Lin, O. F. Wang, and T. C. Chong, J. Appl. Phys. **96**, 6845 (2004).
[14] B. S. Luk'yanchuk, N. Arnold, S. M. Huang, Z. B. Wang, and M. H. Hong, Appl. Phys. A: Mater. Sci. Process. **77**, 209 (2003).
[15] B. S. Luk'yanchuk, Z. B. Wang, W. D. Song, and M. H. Hong, Appl. Phys. A: Mater. Sci. Process. **79**, 747 (2004).